Epilepsy Research 154 (2019) 1–7

Contents lists available at ScienceDirect

Epilepsy Research

journal homepage: www.elsevier.com/locate/epilepsyres

Seizure control by low-intensity ultrasound in mice with temporal lobe epilepsy

Xin Li[a], Huifang Yang[a], Jiaqing Yan[b], Xingran Wang[a], Yi Yuan[a,*], Xiaoli Li[c,*]

[a] Institute of Electrical Engineering, Yanshan University, Qinhuangdao, 066004, China
[b] College of Electrical and Control Engineering, North China University of Technology, Beijing, 10041, China
[c] State Key Laboratory of Cognitive Neuroscience and Learning, Beijing Normal University, Beijing, 100875, China

ABSTRACT

Background: Temporal lobe epilepsy (TLE) is the most common form of focal epilepsy. Recent studies have demonstrated that ultrasound stimulation can inhibit spontaneous recurrent seizures and improve behavioral outcomes for rodents with TLE. However, the exact underlying mechanism for inhibition of TLE via ultrasound stimulation remains unknown.
Methods: In this study, low-intensity pulsed ultrasound stimulation (LIPUS) and low-intensity continuous ultrasound stimulation (LICUS) and concurrent local field potentials (LFPs) in the CA3 field of the hippocampus were recorded in the kainite-induced mouse model of TLE. The power spectrum and the phase-amplitude coupling in the LFPs were quantitatively analyzed.
Results: We found three significant changes in LFPs after ultrasound stimulation: (i) the intensity of the power spectrum in the low frequency (< 10 Hz) was significantly decreased ($p < 0.01$); (ii) the phase amplitude coupling strength between slow (delta-, theta-, and alpha-frequency bands) and fast (gamma frequency bands) neural oscillations were weakened ($p < 0.01$); (iii) the interval between seizures was significantly increased ($p < 0.01$).
Conclusions: These results indicate that the seizures of TLE can be effectively inhibited by ultrasound stimulation, and this effect is independent of ultrasound type (pulsed or continuous).

1. Introduction

Epilepsy, one of the most common neurologic disorders worldwide, is caused by abnormal, highly synchronized discharges from a plurality of neurons (Chang and Lowenstein, 2003; Sen et al., 2018). Repeated epileptic seizures lead to anxiety, depression, accidental disability, and even death, and greatly affect quality of life (Johnson et al., 2004; Keezer et al., 2016; Lambert and Robertson, 1999). TLE is the most common epileptic syndrome in adults and accounts for more than half of refractory epilepsy cases (Krook-Magnuson et al., 2013; Pittau et al., 2012; Wiebe et al., 2002).

In the clinic, epilepsy is mainly treated with antiepileptic drugs, but about 20–30% of patients experience recurrent episodes, which becomes classified as drug-refractory epilepsy (Schmidt and Schachter, 2014; Vyas et al., 2015). In addition, long-term use of antiepileptic drugs can lead to damage of the liver, kidney, and hematopoietic bone marrow, and so some patients cannot tolerate them (Golyala and Kwan, 2016). Surgical treatment may be effective in some patients. However, preoperative evaluation is invasive, and surgery can easily injure unaffected brain areas (Jobst and Cascino, 2015). Previous studies have reported the use of brain stimulation techniques, including deep brain stimulation, optogenetic stimulation, transcranial magnetic stimulation, and transcranial direct-current stimulation, for the inhibition of epileptic seizures (Bidwell et al., 2015; Brunoni et al., 2012; Chiang et al., 2014; Kimiskidis et al., 2014; Zhong et al., 2011). Deep brain stimulation and optogenetic stimulation can accurately and effectively inhibit epileptic seizures; however, deep brain stimulation requires surgical implantation of electrodes and optogenetic stimulation requires modification of the genome and surgical implantation of optical fibers, and therefore both are invasive brain stimulation procedures (Paz and Huguenard, 2014; Yu et al., 2018).

Transcranial magnetic stimulation and transcranial direct-current

Abbreviations: TLE, Temporal lobe epilepsy; LIPUS, low-intensity pulsed ultrasound stimulation; LICUS, low-intensity continuous ultrasound stimulation; LFP, local field potential; PAC, phase-amplitude coupling; PACI, phase-amplitude coupling index; PRF, pulsed repetition frequency; SD, stimulation duration; FF, fundamental frequency; DC, duty cycle; KA, kainite; Pre-Stim, pre-stimulation; Stim-On, stimulation-on; Post-Stim, post-stimulation; KA group, KA injected group; KA + LIPUS group, KA injected mice with low-intensity pulsed ultrasound stimulation group; KA + LICUS group, KA injected mice with low-intensity continuous ultrasound stimulation group; AP, anterior-posterior; ML, medial-lateral; DV, dorsal-ventral

* Corresponding author.
E-mail addresses: yuanyi513@ysu.edu.cn (Y. Yuan), xiaoli@bnu.edu.cn (X. Li).

https://doi.org/10.1016/j.eplepsyres.2019.04.002
Received 27 November 2018; Received in revised form 23 March 2019; Accepted 3 April 2019
Available online 04 April 2019
0920-1211/

stimulation can noninvasively and effectively suppress seizures, but their spatial resolution and penetration depth are low (Pereira et al., 2016; San-Juan et al., 2015). Recent years have seen the rapid development of low-intensity ultrasound stimulation, which has the advantages of higher spatial resolution and greater penetration depth, and has emerged as a new modality for noninvasive neuromodulation (Bystritsky et al., 2011; Landhuis, 2017). The potential mechanisms of ultrasound stimulation for neuromodulation may be that ultrasound wave alter intramembrane cavitation, membrane conductance or mechanically sensitive ion channels to cause neuronal discharge (Plaksin et al., 2014; Tyler, 2011; Ye et al., 2018). Previous studies have shown that ultrasound stimulation can be used to safely modulate brain activity in patients with and animal models of neuropsychiatric diseases, including ischemic stroke (Chen et al., 2018a; Li et al., 2017), Alzheimer's disease and dementia (Eguchi et al., 2018; Lin et al., 2015), traumatic brain injury (Chen et al., 2018b; Monti et al., 2016; Su et al., 2017), and depression (Zhang et al., 2018). More recently, ultrasound stimulation has been used to inhibit epilepsy; Min et al. investigated the feasibility of ultrasound stimulation to non-invasively suppress a pentylenetetrazol-induced rat model of epilepsy (Min et al., 2011). The authors found that ultrasound stimulation applied to a rat model of epilepsy resulted in few occurrences of epileptic EEG bursts and less severe epileptic behavior. Hakimova et al. utilized pulsed ultrasound to stimulate a KA-induced mouse model of mesial TLE during the initial acute period (Hakimova et al., 2015; Min et al., 2011). The mice with ultrasound stimulation in the initial period exhibited fewer spontaneous recurrent seizures and improved performance in behavioral tasks assessing sociability and depression in the chronic period of epilepsy (Hakimova et al., 2015; Min et al., 2011). Thus, ultrasound stimulation can effectively inhibit epileptic seizures.

With the advantages of non-invasiveness and spatial selectivity, low-intensity ultrasound stimulation may provide new perspectives for possible therapies in patients with epilepsy. In this study, mice with KA-induced TLE received LIPUS or LICUS, and the power spectrum and PAC of LFPs were recorded and analyzed in the Pre-Stim, Stim-On, and Post-Stim phases.

2. Methods

2.1. Animals

Thirty-seven C57BL/6 mice were used in the experiments (all male, body weight 20–25 g, Beijing Vital River Laboratory Animal Technology Co., Ltd. China). All procedures were conducted according to the Animal Ethics and Administrative Council of Yanshan University. The mice were housed in standard cages in a 12-hour light/dark cycle and had *ad libitum* access to food and water. The mice were randomly divided into three groups, including a KA group (N = 6), KA + LIPUS group (N = 8), and KA + LICUS group (N = 8). Additional fifteen mice were used for measuring the latency to seizure. Body temperature was maintained at ˜37 ˚C using a closed-loop animal temperature maintenance instrument (69002, Ruiwode, Shenzhen, China) during all experiments.

2.2. The TLE mouse model and electrode implantation

The TLE mouse model was generated according to previous work (Min et al., 2011). Surgical anesthesia for all mice was induced with 2% isoflurane, and oxygen was continuously delivered at 2 L per min. The anesthetized mice were fixed on a mouse adapter (68030, Ruiwode, Shenzhen, China) with ear bars and a clamping device. KA (1 μg/1 μl in saline, Tocris, USA) was unilaterally microinfused into the CA3 area (AP = -2.0 mm, ML = -2.3 mm, and DV = 2.0 mm from bregma) via a needle (33 gauge, NanoFil, World Precision Instruments, USA) connected to a 25-μl Hamilton syringe; the flow rate (0.05 μl min^{-1}) was regulated by a syringe pump (SP101i, World Precision Instruments, USA). After the injection, we left the needle for 5 min to prevent leakage before slowly pulling it out. Tungsten microelectrodes (WE50030.1B10, MicroProbe, USA) were inserted into the CA3 region (AP = -2.0 mm, ML = -2.3 mm, and DV = 2.0 mm from bregma) 2 h after generation of the TLE model. A reference screw electrode and a ground screw electrode were inserted into the nasal bone. 1.75% isoflurane (RWD Life Science Co. Shenzhen, China) and oxygen were continuously delivered at 2 L per min to anesthetized mice for subsequent ultrasound stimulation and LFPs recording experiments.

2.3. Low-intensity ultrasound stimulation protocol

LIPUS and LICUS were used in our experiments. With LIPUS, two connected function generators (AFG3022C; Tektronix, USA) were used to generate pulsed signals. The first function generator, which generated square waves to trigger the operation of the second function generator, was used to control the PRF and SD. The second function generator was used to control the FF, DC, and acoustic intensity. As shown in Fig. 1, the FF, PRF, DC, and SD of pulsed ultrasound were 500 kHz, 500 Hz, 50% and 30 s, respectively (Hakimova et al., 2015; Yusuf et al., 2010). With LICUS, the continuous sine wave was generated by a function generator. The FF and SD of the continuous ultrasound were 500 kHz and 30 s. The pulsed signal or continuous signal was amplified by a linear power amplifier (E&I240 L, ENI Inc., USA) and transmitted to an unfocused ultrasound transducer (V301-SU, Olympus, USA). The ultrasound transducer had a single element with diameter of 25.4 mm, and was connected to the skull by a conical collimator that was filled with ultrasound coupling gel. The diameter of the hole at the bottom of the conical collimator was 2 mm. The two-dimensional ultrasound distribution in xz, yz, and xy planes (Fig. 2) was measured using a calibrated needle-type hydrophone (HNR500; Onda, USA) that was moved by a two-dimensional electric translation platform. The maximum ultrasound pressure of both pulsed and continuous ultrasound was 0.26 MPa.

2.4. LFP signal recording

The microelectrode recorded the LFP signals using a dual-channel pre-amplifier (63386, A-M Systems Inc., USA). The analog signals were converted into digital signals using a 32-channel neural signal processor (Cerebus Data Acquisition System, Blackrock Microsystems, USA), which were then transmitted to a computer for data storage and processing. Raw LFP signals were acquired at a sampling frequency of 2 kHz, and a low-pass filter with a 1000-Hz cutoff frequency was set in the differential pre-amplifier system.

2.5. Ultrasound stimulation sequence

To verify that ultrasound stimulation can inhibit seizures in TLE, we recorded LFPs from the CA3 region of mice in KA, KA + LIPUS, and

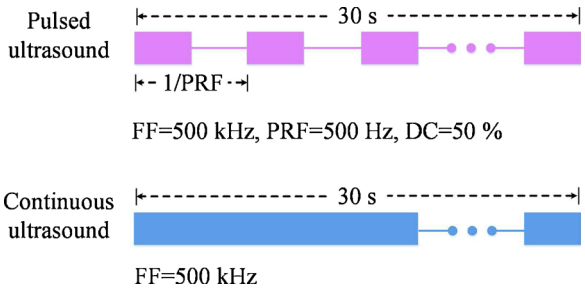

Fig. 1. Experimental time sequence. (A) The time sequence of the LIPUS and LICUS. The ultrasound FF, PRF, DC, and SD were 500 kHz, 500 Hz, 50%, and 30 s with LIPUS. The FF and SD were 500 kHz and 30 s with LICUS. (B) The two-dimensional ultrasound distribution in xz, yz, and xy planes.

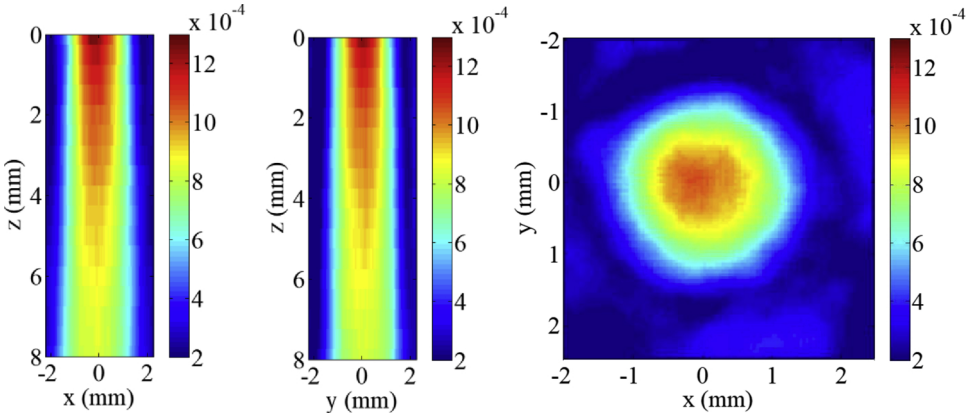

Fig. 2. Ultrasound distribution. The two-dimensional ultrasound distribution in xz, yz, and xy planes.

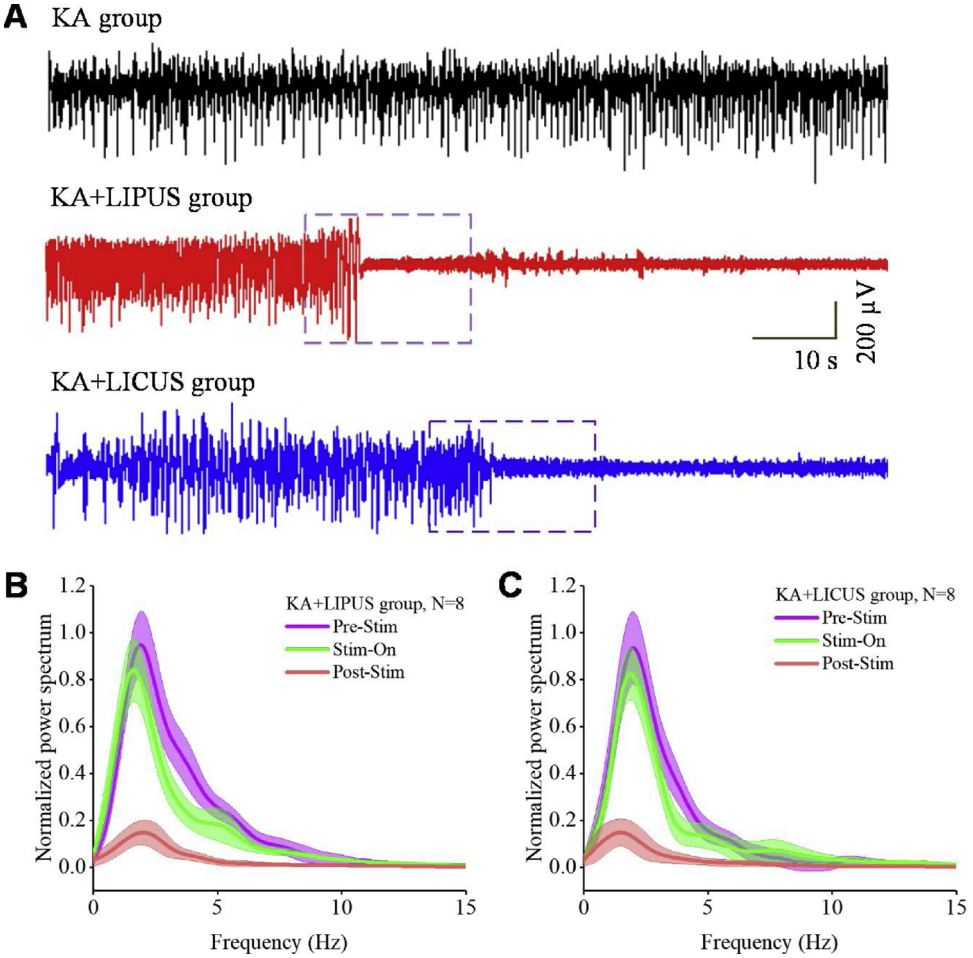

Fig. 3. Ultrasound stimulation modulates the LFP power spectrum in TLE. (A) LFPs in the KA, KA + LIPUS, and KA + LICUS groups. Ultrasound stimulation (30 s) is marked by a purple dotted frame, and is shown for both KA + LIPUS and KA + LICUS groups. (B) and (C) LFP power spectrum at Pre-Stim, Stim-On, and Post-Stim phases in the KA + LIPUS (D) and KA + LICUS (E) groups. The power spectrum intensity was mainly concentrated to low frequencies (< 10 Hz) during seizures (Pre-Stim). The peak intensity of the power spectrum dropped significantly and reduced to ˜20% of that in the Pre-Stim phase in the KA + LIPUS and KA + LICUS groups.

KA + LICUS groups. We defined seizures with LFP according to the previous literature (Amplitude: 3 × background, Lasting time: > 10 s) (Hakimova et al., 2015). Data was analyzed to detect seizures in real-time. Detection threshold was set at approximately three times the amplitude of the background signal. We setup a threshold value approximately equal to three times the amplitude of background signal in the recording software. When the amplitude of the LFPs was above the threshold line and the seizures lasted more than 30 s, we manually turned on the trigger switch of ultrasound stimulation for 30 s.

The LFPs were continuously recorded for 100 s in the KA group once we had confirmed seizures. In the KA + LIPUS and KA + LICUS groups, we began recording LFPs once we had confirmed seizures. The total recording time was also 100 s in the KA + LIPUS and KA + LICUS groups. In the series of experiments for measuring the latency to the next seizure, we recorded the LFPs until the occurrence of the next seizure in KA group (N = 5), KA + LIPUS group (N = 5) and

KA + LICUS group (N = 5). Five seizures were tried for each mouse.

2.6. Data analysis

The Welch algorithm was used to analyze the power spectrum of LFPs with data segments, adding windows function, and averaging data. We set the window to a Hamming window with a width of 30,000 points and an overlap of 29,000 points. The parameters used for measuring oscillatory activity was the peak frequency (Hz) and the mean absolute power (μV^2/Hz). We used PACI, that is the index of the Pac strength.

We modified Voytek's method (Voytek et al., 2013) to calculate the PACI for low and high frequency bands and it is defined by formula (1):

$$PACI = \left| \frac{1}{K} \sum_{k=1}^{K-1} \exp(i(\phi_l[k] - \phi_h[k])) \right| \quad (1)$$

where PACI is the phase-locking value between ongoing ϕ_l and ϕ_k, and k is the time index. ϕ_l is the phase of low-frequency oscillation, ϕ_k is the phase of the high-frequency oscillation filtered by low-frequency band-pass filter. The higher the PACI, the stronger the Pac strength.

2.7. Statistical analysis

Pre-Stim, Stim-on, and Post-Stim comparisons were made using the Kruskal-Wallis test, and differences were deemed significant if $p < 0.05$. The statistical analysis was performed using Matlab software.

3. Results

3.1. Ultrasound stimulation modulates the LFP power spectrum in TLE

Fig. 3A shows the LFPs in the KA, KA + LIPUS, and KA + LICUS groups. Ultrasound stimulation (30 s) in the KA + LIPUS and KA + LICUS groups is marked by a purple dotted frame. In the KA + LIPUS and KA + LICUS groups, ultrasound stimulation of CA3 inhibited the seizure in Stim-On, and the seizure of TLE was completely suppressed in Post-Stim. Next, we performed a quantitative analysis of spike frequency and power spectrum of LFPs in Pre-Stim, Stim-On, and Post-Stim in the KA + LIPUS and KA + LICUS groups. Then, we calculated the power spectrum of LFPs in the Pre-Stim (30 s), Stim-On (30 s), and Post-Stim (30 s) phases in the KA + LIPUS and KA + LICUS groups. Power spectrum data were normalized to allow for comparisons as shown in Fig. 3B (KA + LIPUS group) and 3C (KA + LICUS group), the intensity of the power spectrum was mainly concentrated at the low frequency (< 10 Hz) during seizures (Pre-Stim). While ultrasound stimulation resulted in a decrease in the peak intensity of the power spectrum, this change was not obvious in either the KA + LIPUS or KA + LICUS groups. This may be because the epileptic seizure was not immediately inhibited following stimulation, and the abnormal discharge therefore continued during Stim-On. The peak intensity of the power spectrum dropped during Stim-On to around 20% of that in the Pre-Stim phase in both the KA + LIPUS and KA + LICUS groups. The change in power spectrum intensity indicates that ultrasound stimulation inhibits slow neural oscillations of seizure activity in TLE.

Fig. 4A shows the spike frequency in the Pre-Stim, Stim-On, and Post-Stim phases in the KA + LIPUS and KA + LICUS groups. We chose the spikes according to the reference (Amplitude: 3 × background) (Hakimova et al., 2015) and the spike frequency is the number of spikes per unit time. (unit: Hz). Compared to Pre-Stim, the spike frequency decreased in the Stim-On phase and was significantly reduced at Post-Stim for both the KA + LIPUS (mean values from five seizures of each mouse over eight mice, Pre-Stim: 1.15 ± 0.21 Hz; Stim-On: 0.66 ± 0.17 Hz; Post-Stim: 0.01 ± 0.01 Hz, Kruskal-Wallis test, $p < 0.01$) and KA + LICUS groups (mean values from five seizures of each mouse over eight mice, Pre-Stim: 1.15 ± 0.21 Hz; Stim-On: 0.77 ± 0.16 Hz; Post-Stim: 0.02 ± 0.01 Hz, Kruskal-Wallis test, $p < 0.01$). To obtain the latency to the next seizure, we continuously recorded the LFPs until the next seizure in fifteen additional mice from the KA group (N = 5), KA + LIPUS group (N = 5) and KA + LICUS group (N = 5).

We measured the interval between two adjacent seizures for each of 5 seizures per mouse in KA, KA + LIPUS, and KA + LICUS groups. As shown in Fig. 4B, the onset of next seizure was delayed by 96.6 ± 18.5 s in the KA group (mean values from five seizures across five mice per mouse ± standard error of the mean), 383.2 ± 51.6 s in the KA + LIPUS group, and 378.6 ± 60.8 s in the KA + LICUS group (Kruskal-Wallis test, $p < 0.01$). The results showed that the interval to next seizure were lengthened following a 30 s ultrasound stimulation at the occurrence of the first seizure. These results demonstrate that low-intensity ultrasound stimulation can effectively inhibit seizure activity of TLE; in addition, there was no significant difference between the inhibition effects of LIPUS and LICUS.

3.2. Ultrasound stimulation modulates PAC strength of LFPs in TLE

Considering that ultrasound stimulation suppressed slow oscillations of TLE seizures, and that PAC between slow and fast neural oscillations has been reported to be an important characteristic of LFPs in TLE (Edakawa et al., 2016; Lopezpigozzi et al., 2016; Samiee et al., 2018), we investigated the relationship between the ultrasound stimulation-induced inhibition of TLE and PAC of slow-fast neural oscillations. First, we determined the coupling strength of slow-fast neural oscillations by examining PAC in the KA + LIPUS and KA + LICUS groups. As shown in Fig. 5A, there was a clear correspondence between the trough of slow oscillations and the peak of fast oscillations in Pre-Stim; this correspondence was weaker in Stim-On and hardly visible in Post-Stim. Fig. 5B shows PACI images as a function of the analytic phase (1–20 Hz) and analytic amplitude (1–45 Hz) for Pre-Stim, Stim-On, and Post-Stim in the KA + LIPUS and KA + LICUS groups. In Pre-Stim, the PACI value had a strong coupling between slow and fast neural oscillations during seizures. Compared to Pre-Stim, the coupling between alpha (8–13 Hz) and gamma (30–45 Hz) frequencies significantly decreased in Stim-On. In Post-Stim, the coupling between delta (1–4 Hz), theta (4–8 Hz), alpha, and gamma frequencies was reduced after ultrasound stimulation in both the KA + LIPUS and KA + LICUS groups. In particular, ultrasound stimulation reduced the coupling between alpha and gamma more rapidly. One previous study found that LFPs in epilepsy are primarily composed of delta and gamma frequency bands, which manifest as slow and fast oscillations, respectively (Weiss et al., 2013; Zhang et al., 2017). Our results demonstrate that the pathological function of LFPs in delta-, theta-, alpha- and gamma frequency bands is reduced by ultrasound stimulation.

Furthermore, we quantitatively computed the mean PACI between slow and fast neural oscillations, including delta-gamma, theta-gamma, and alpha-gamma. The mean PACI for each group is shown in Fig. 6A–C. As shown in Fig. 6A, the mean PACI between delta and gamma bands in Pre-Stim, Stim-On, and Post-Stim were 0.41 ± 0.04, 0.33 ± 0.05, and 0.26 ± 0.03 in the KA + LIPUS group and 0.39 ± 0.05, 0.32 ± 0.05, and 0.28 ± 0.03 in the KA + LICUS group. Compared to Pre-Stim, the PACI in Post-Stim was significantly decreased by ˜1.6 times and ˜1.4 times in the KA + LIPUS and KA + LICUS groups, respectively (mean values from five seizures of each mouse over eight mice, Kruskal-Wallis test, Stim-On vs. Pre-Stim: $p < 0.05$, Post-Stim vs. Pre-Stim: $p < 0.05$). The mean Pac indices between theta and gamma bands in Pre-Stim, Stim-On, and Post-Stim were 0.33 ± 0.04, 0.31 ± 0.05, and 0.19 ± 0.03 in the KA + LIPUS group and 0.34 ± 0.05, 0.29 ± 0.04, and 0.20 ± 0.02 in the KA + LICUS group. Compared to the Pre-Stim phase, the Post-Stim mean Pac indices decreased by ˜1.7 times in both the KA + LIPUS and KA + LICUS groups (mean values from five seizures of each mouse over eight mice, Kruskal-Wallis test, Stim-On vs. Pre-Stim: $p < 0.05$, Post-Stim vs.

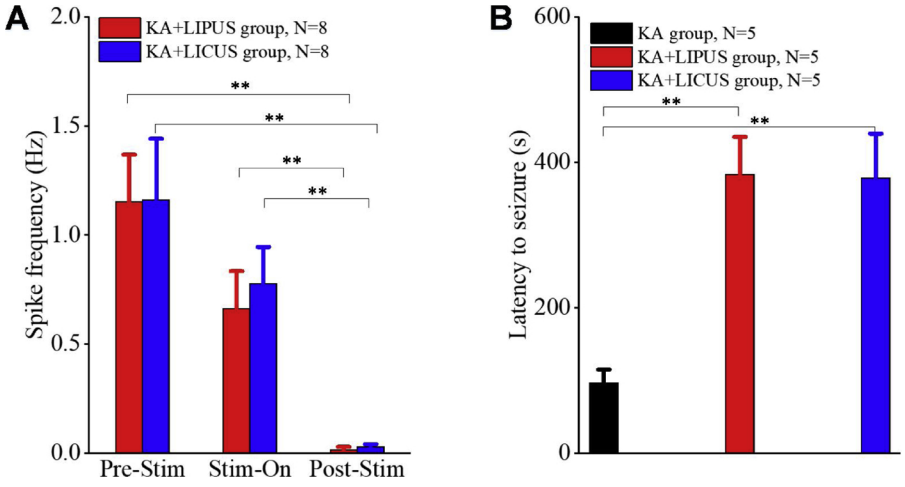

Fig. 4. Ultrasound stimulation modulates spike frequency and the latency to seizure in TLE. (A) Spike frequency in the Pre-Stim, Stim-On, and Post-Stim phases for the KA + LIPUS and KA + LICUS groups. (mean values from five seizures of each mouse over eight mice, Pre-Stim: 1.15 ± 0.21 Hz; Stim-On: 0.66 ± 0.17 Hz; Post-Stim: 0.01 ± 0.01 Hz; Kruskal-Wallis test, $^{**}p < 0.01$) and KA + LICUS groups (mean values from five seizures of each mouse over eight mice, Pre-Stim: 1.15 ± 0.21 Hz, Stim-On: 0.77 ± 0.16 Hz, Post-Stim: 0.02 ± 0.01 Hz, Kruskal-Wallis test, $^{**}p < 0.01$). (B) The latency to seizure in KA group (N = 5), KA + LIPUS group (N = 5) and KA + LICUS group (N = 5) (mean values from five seizures of each mouse over all mice, Kruskal-Wallis test, $^{**}p < 0.01$).

Pre-Stim: $p < 0.05$; Fig. 6B). A similar result was found for alpha-gamma coupling at Pre-Stim, Stim-On, and Post-Stim phases (KA + LIPUS group: 0.26 ± 0.04, 0.18 ± 0.03, and 0.14 ± 0.02; KA + LICUS group: 0.27 ± 0.03, 0.21 ± 0.03, and 0.13 ± 0.02; Fig. 6C). The mean PACI between alpha and gamma bands in the Post-Stim phase decreased to ˜1.8 and ˜2.1 times that seen in Pre-Stim for the KA +

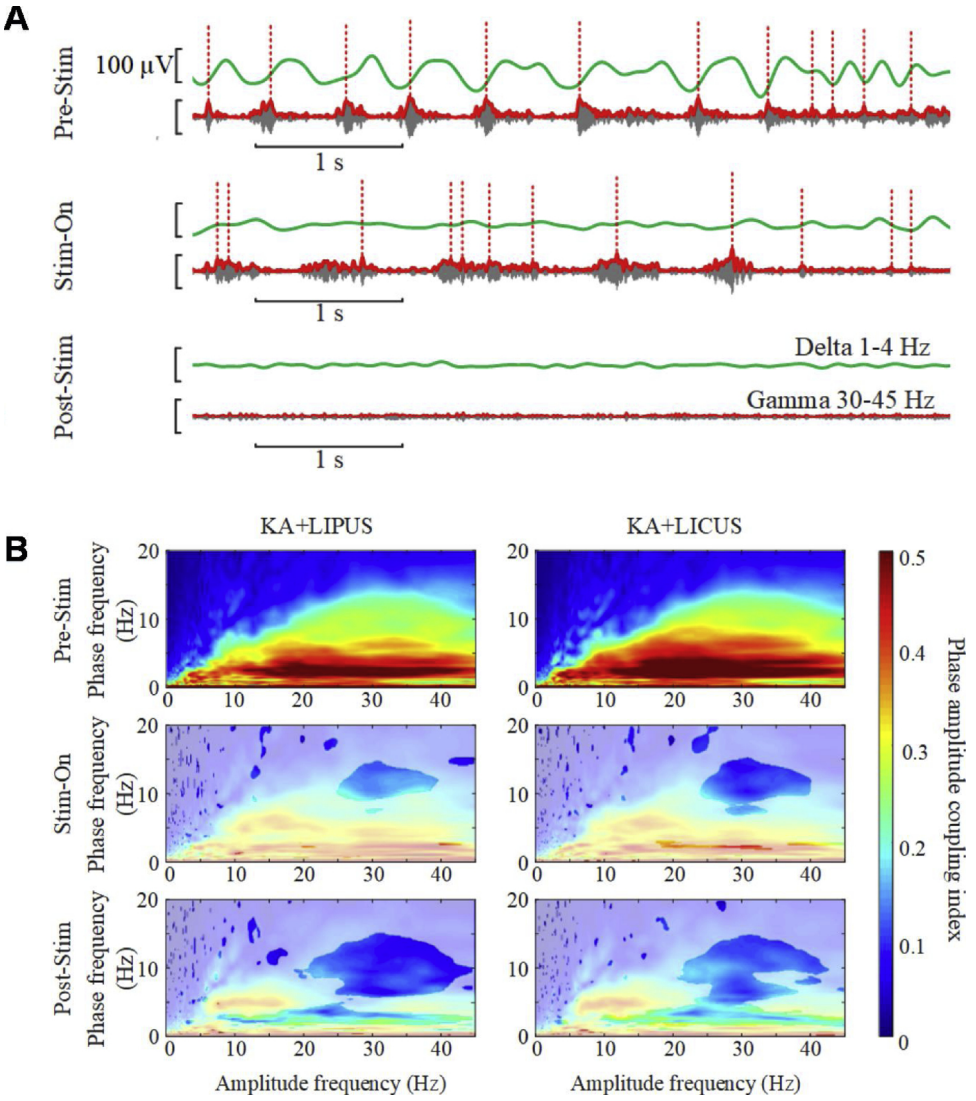

Fig. 5. Ultrasound stimulation modulates PAC strength of LFPs in TLE. (A) The correspondence between the trough of slow oscillations and peak of fast oscillations at the Pre-Stim, Stim-On, and Post-Stim phases (B) PACI images as a function of the analytic phase (1–20 Hz) and analytic amplitude (1–45 Hz) for Pre-Stim, Stim-On, and Post-Stim phases in the KA + LIPUS and KA + LICUS groups.

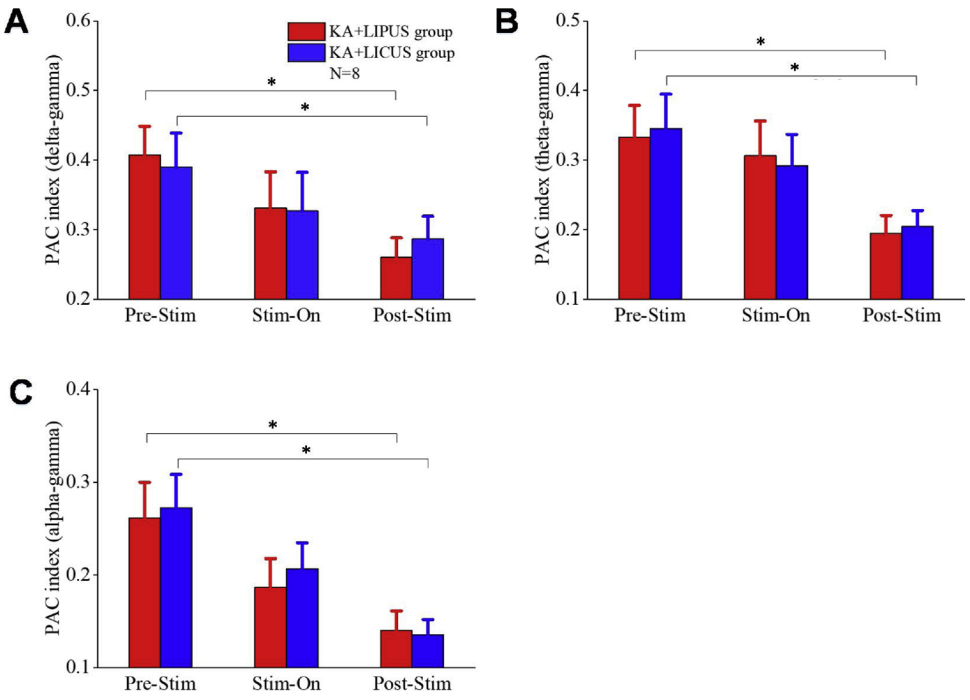

Fig. 6. PACI between delta/theta/alpha and gamma bands. (A) The mean PAC indices between delta and gamma bands in the Pre-Stim, Stim-On, and Post-Stim phases were 0.41 ± 0.04, 0.33 ± 0.05, and 0.26 ± 0.03 in the KA + LIPUS group and 0.39 ± 0.05, 0.32 ± 0.05, and 0.28 ± 0.03 in the KA + LICUS group (mean values from five seizures of each mouse over eight mice, Kruskal-Wallis test, *p < 0.05). (B) The mean PAC indices between theta and gamma bands in the Pre-Stim, Stim-On, and Post-Stim phases were 0.33 ± 0.04, 0.31 ± 0.05, and 0.19 ± 0.03 in the KA + LIPUS group and 0.34 ± 0.05, 0.29 ± 0.04, and 0.20 ± 0.02 in the KA + LICUS group (mean values from five seizures of each mouse over eight mice, Kruskal-Wallis test, *p < 0.05). (C) The mean PACIs in Post-Stim phase between the alpha and gamma bands (mean values from five seizures of each mouse over eight mice, KA + LIPUS group: 0.26 ± 0.04, 0.18 ± 0.03, and 0.14 ± 0.02; KA + LICUS group: 0.27 ± 0.03, 0.21 ± 0.03, and 0.13 ± 0.02, N = 8, Kruskal-Wallis test, *p < 0.05).

LIPUS and KA + LICUS groups, respectively (mean values from five seizures of each mouse over eight mice, Kruskal-Wallis test, Stim-On vs. Pre-Stim: $p < 0.05$, Post-Stim vs. Pre-Stim: $p < 0.05$). Thus, ultrasound stimulation significantly decreased PACI in the delta-gamma, theta-gamma, and alpha-gamma bands. This indicates that ultrasound stimulation caused an obvious decoupling of slow-fast neural oscillations in seizure activity. This decoupling of slow-fast oscillations may underlie the inhibitory effect of ultrasound stimulation on seizures in TLE. The effect of decoupling was not significantly different between the KA + LIPUS and KA + LICUS groups.

4. Discussion

In this study, we applied LIPUS and LICUS to the CA3 region to measure the effect on a model of TLE, and simultaneously recorded LFPs elicited from the CA3 region. The power spectrum and PAC of LFPs during the Pre-Stim, Stim-On, and Post-Stim phases were quantitatively analyzed to reveal the mechanism of ultrasound-induced inhibition of seizure activity in TLE. Our results demonstrate that low-intensity ultrasound can suppress the bursts and slow frequency dynamics, which then results in a drop in PAC. To our knowledge, this is the first report to investigate the power spectrum and PAC of LFPs from ultrasound-induced inhibition of seizures. These findings provide a basis for the potential clinical use of ultrasound stimulation in the treatment of TLE.

A previous study demonstrated that low-intensity ultrasound stimulation can evoke neuron activity by activating voltage-gated sodium channels, voltage-gated calcium channels, or intramembrane cavitation within the bilayer membrane in neurons (Tyler et al., 2018). We think that ultrasound stimulation may affect slow and fast neural oscillations, destroy the synchronous discharge rhythm of epilepsy and inhibit epileptic discharge based on the above potential mechanisms.

In our study, ictal and postictal periods could be encountered within the preset ultrasound stimulation periods and the precise timing of seizures abatement under ultrasound stimulation within those periods appeared to be random. Similar results were also shown in previous work by Hakimova et al (Hakimova et al., 2015). In order to work with the same data length in subsequent mathematical analysis, we did not separate seizure and post-seizure periods during stimulation periods, but we analyzed the changes of LFP at the preset peri-ultrasound stimulation periods, that is, pre-stim: 30 s, stim-on: 30 s, post-stim: 30 s.

Changes in physiological parameters by ultrasound stimulation have not been investigated (Hakimova et al., 2015; Min et al., 2011). In a future study, we plan to address this question and reveal potential molecular mechanisms of ultrasound stimulation in the abatement of seizures.

5. Conclusions

In summary, our study indicates that ultrasound stimulation can effectively inhibit seizures of TLE. This inhibition effect is independent of ultrasound type (pulsed and continuous ultrasound).

Conflict of interest

The authors declare no competing financial interests.

Acknowledgements

This research was supported by National Natural Science Foundation of China (61827811, 61673336, 61503321), Key Project of Natural Science Foundation of Hebei Province (F2018203256).

References

Bidwell, J., Khuwatsamrit, T., Askew, B., Ehrenberg, J.A., Helmers, S., 2015. Seizure reporting technologies for epilepsy treatment: a review of clinical information needs and supporting technologies. Seizure Eur. J. Epilepsy 32, 109–117.

Brunoni, A.R., Nitsche, M.A., Bolognini, N., Bikson, M., Wagner, T., Merabet, L., Edwards, D.J., Valerocabre, A., Rotenberg, A., Pascualleone, A., 2012. Clinical research with transcranial direct current stimulation (tDCS): challenges and future directions. Brain Stimul. 5, 175–195.

Bystritsky, A., Korb, A.S., Douglas, P.K., Cohen, M.S., Melega, W.P., Mulgaonkar, A.P., Desalles, A., Min, B.K., Yoo, S.S., 2011. A review of low-intensity focused ultrasound pulsation. Brain Stimul. 4, 125–136.

Chang, B.S., Lowenstein, D.H., 2003. Epilepsy. N. Engl. J. Med. 349, 1257.

Chen, C.M., Wu, C.T., Yang, T.H., Liu, S.H., Yang, F.Y., 2018a. Preventive effect of low intensity pulsed ultrasound against experimental cerebral ischemia/reperfusion injury via apoptosis reduction and brain-derived neurotrophic factor induction. Sci. Rep. 8, 5568.

Chen, S.F., Su, W.S., Wu, C.H., Lan, T.H., Yang, F.Y., 2018b. Transcranial ultrasound stimulation improves long-term functional outcomes and protects against brain

damage in traumatic brain injury. Mol. Neurobiol. 55, 7079–7089.
Chiang, C.C., Ladas, T.P., Gonzalezreyes, L.E., Durand, D.M., 2014. Seizure suppression by high frequency optogenetic stimulation using in vitro and in vivo animal models of epilepsy. Brain Stimul. 7, 890–899.
Edakawa, K., Yanagisawa, T., Kishima, H., Fukuma, R., Oshino, S., Hui, M.K., Kobayashi, M., Tanaka, M., Yoshimine, T., 2016. Detection of epileptic seizures using phase–amplitude coupling in intracranial electroencephalography. Sci. Rep. 6, 25422.
Eguchi, K., Shindo, T., Ito, K., Ogata, T., Kurosawa, R., Kagaya, Y., Monma, Y., Ichijo, S., Kasukabe, S., Miyata, S., 2018. Whole-brain low-intensity pulsed ultrasound therapy markedly improves cognitive dysfunctions in mouse models of dementia - Crucial roles of endothelial nitric oxide synthase. Brain Stimul. 11, 959–973.
Golyala, A., Kwan, P., 2016. Drug development for refractory epilepsy: the past 25 years and beyond. Seizure 44, 147–156.
Hakimova, H., Kim, S., Chu, K., Sang, K.L., Jeong, B., Jeon, D., 2015. Ultrasound stimulation inhibits recurrent seizures and improves behavioral outcome in an experimental model of mesial temporal lobe epilepsy. Epilepsy Behav. 49, 26–32.
Jobst, B.C., Cascino, G.D., 2015. Resective epilepsy surgery for drug-resistant focal epilepsy: a review. Jama 313, 285.
Johnson, E.K., Jones, J.E., Seidenberg, M., Hermann, B.P., 2004. The relative impact of anxiety, depression, and clinical seizure features on health-related quality of life in epilepsy. Epilepsia 45, 544–550.
Keezer, M.R., Sisodiya, S.M., Sander, J.W., 2016. Comorbidities of epilepsy: current concepts and future perspectives. Lancet Neurol. 15, 106–115.
Kimiskidis, V.K., Valentin, A., Kälviäinen, R., 2014. Transcranial magnetic stimulation for the diagnosis and treatment of epilepsy. Curr. Opin. Neurol. 27, 236–241.
Krook-Magnuson, E., Armstrong, C., Oijala, M., Soltesz, I., 2013. On-demand optogenetic control of spontaneous seizures in temporal lobe epilepsy. Nat. Commun. 4, 1376.
Lambert, M.V., Robertson, M.M., 1999. Depression in epilepsy: etiology, phenomenology, and treatment. Epilepsia 40, 21–47.
Landhuis, E., 2017. Ultrasound for the brain. Nature 551, 257.
Li, H., Sun, J., Zhang, D., Omiremayor, D., Lewin, P.A., Tong, S., 2017. Low-intensity (400 mW/cm^2, 500 kHz) pulsed transcranial ultrasound preconditioning may mitigate focal cerebral ischemia in rats. Brain Stimul. 10, 695–702.
Lin, W.T., Chen, R.C., Lu, W.W., Liu, S.H., Yang, F.Y., 2015. Protective effects of low-intensity pulsed ultrasound on aluminum-induced cerebral damage in Alzheimer's disease rat model. Sci. Rep. 5, 9671.
Lopezpigozzi, D., Laurent, F., Brotonsmas, J.R., Valderrama, M., Valero, M., Fernandezlamo, I., Cid, E., Gomezdominguez, D., Gal, B., Prida, L.M.D.L., 2016. Altered oscillatory dynamics of CA1 parvalbumin basket cells during theta–gamma rhythmopathies of temporal lobe epilepsy. eNeuro 3.
Min, B.K., Bystritsky, A., Jung, K.I., Fischer, K., Zhang, Y., Maeng, L.S., Sang, I.P., Chung, Y.A., Jolesz, F.A., Yoo, S.S., 2011. Focused ultrasound-mediated suppression of chemically-induced acute epileptic EEG activity. BMC Neurosci. 12, 23.
Monti, M.M., Schnakers, C., Korb, A.S., Bystritsky, A., Vespa, P.M., 2016. Non-invasive ultrasonic thalamic stimulation in disorders of consciousness after severe brain injury: a first-in-man report. Brain Stimul. 9, 940–941.
Paz, J.T., Huguenard, J.R., 2014. Optogenetics and epilepsy: past, present and future. Epilepsy Curr. 15, 34–38.
Pereira, L.S., Müller, V.T., Da, M.G.M., Rotenberg, A., Fregni, F., 2016. Safety of repetitive transcranial magnetic stimulation in patients with epilepsy: a systematic review. Epilepsy Behav. 57, 167–176.
Pittau, F., Grova, C., Moeller, F., Dubeau, F., Gotman, J., 2012. Patterns of altered functional connectivity in mesial temporal lobe epilepsy. Epilepsia 53, 1013–1023.
Plaksin, M., Shoham, S., Kimmel, E., 2014. Intramembrane cavitation as a predictive bio-piezoelectric mechanism for ultrasonic brain stimulation. Physical review X 4, 011004.
Samiee, S., Lévesque, M., Avoli, M., Baillet, S., 2018. Phase-amplitude coupling and epileptogenesis in an animal model of mesial temporal lobe epilepsy. Neurobiol. Dis. 114, 111–119.
San-Juan, D., Morales-Quezada, L., Garduño, A.J.O., Alonso-Vanegas, M., López, D.A.E., Gregorio, R.V., Anschel, D.J., Fregni, F., 2015. Transcranial direct current stimulation in epilepsy. Brain Stimul. 8, 455–464.
Schmidt, D., Schachter, S.C., 2014. Drug treatment of epilepsy in adults. Bmj 348 g254.
Sen, A., Capelli, V., Husain, M., 2018. Cognition and dementia in older patients with epilepsy. Brain J. Neurol. 141, 1592.
Su, W.S., Wu, C.H., Chen, S.F., Yang, F.Y., 2017. Transcranial ultrasound stimulation promotes brain-derived neurotrophic factor and reduces apoptosis in a mouse model of traumatic brain injury. Brain Stimul. 10, 1032–1041.
Tyler, W.J., 2011. Noninvasive neuromodulation with ultrasound? A continuum mechanics hypothesis,Neuroscientist. A Review Journal Bringing Neurobiology Neurology and Psychiatry 1 (17), 25.
Tyler, W.J., Lani, S.W., Hwang, G.M., 2018. Ultrasonic modulation of neural circuit activity. Curr. Opin. Neurobiol. 50, 222–231.
Voytek, B., D'Esposito, M., Crone, N., Knight, R.T., 2013. A method for event-related phase/amplitude coupling. Neuroimage 64, 416–424.
Vyas, M.V., Davidson, B.A., Escalaya, L., Costella, J., Saposnik, G., Burneo, J.G., 2015. Antiepileptic drug use for treatment of epilepsy and dyslipidemia: systematic review. Epilepsy Res. 113, 44–67.
Weiss, S.A., Banks, G.P., Mckhann, G.M., Goodman, R.R., Emerson, R.G., Trevelyan, A.J., Schevon, C.A., 2013. Ictal high frequency oscillations distinguish two types of seizure territories in humans. Brain 136, 3796–3808.
Wiebe, S., Blume, W.T., Girvin, J.P., Eliasziw, M., Butler, J.T., Mcinnis, W.P., Mclachlan, R.S., Young, G.B., Parrent, A., Sahjpaul, R., 2002. A randomized, controlled trial of surgery for temporal-lobe epilepsy. N. Engl. J. Med. 345, 311–318.
Ye, J., Tang, S.Y., Meng, L., Li, X., Wen, X.X., Chen, S.H., Niu, L.L., Li, X.Y., Qiu, W.B., Hu, H.L., Jiang, M.Z., Shang, S.Q., Qiang, S., Zheng, H.R., Duan, S.M., Li, Y.Z., 2018. Ultrasonic control of neural activity through activation of the mechanosensitive channel mscl. Nano Letters 18, 4148–4155.
Yu, T., Wang, X., Li, Y., Zhang, G., Worrell, G., Chauvel, P., Ni, D., Qiao, L., Liu, C., Li, L., 2018. High-frequency stimulation of anterior nucleus of thalamus desynchronizes epileptic network in humans. Brain 141, 2631–2643.
Yusuf, T., Alexei, M., Nathan, B., Tauchmann, M.L., Joseph, G., Anna, Y., Tillery, S.I.H., Tyler, W.J., 2010. Transcranial pulsed ultrasound stimulates intact brain circuits. Neuron 66, 681–694.
Zhang, R., Ren, Y., Liu, C., Xu, N., Li, X., Cong, F., Ristaniemi, T., Wang, Y., 2017. Temporal-spatial characteristics of phase-amplitude coupling in electrocorticogram for human temporal lobe epilepsy. Clin. Neurophysiol. 128, 1707–1718.
Zhang, D., Li, H., Sun, J., Hu, W., Jin, W., Li, S., Tong, S., 2018. Antidepressant-like effect of low-intensity transcranial ultrasound stimulation. IEEE Trans. Biomed. Eng. 66, 411–420.
Zhong, X.L., Yu, J.T., Zhang, Q., Wang, N.D., Tan, L., 2011. Deep brain stimulation for epilepsy in clinical practice and in animal models. Brain Res. Bull. 85, 81–88.